Chinese Chemical Letters 35 (2024) 108626

Contents lists available at ScienceDirect

Chinese Chemical Letters

journal homepage: www.elsevier.com/locate/cclet

Supramolecular cyclization induced emission enhancement in a pillar[5]arene probe for discrimination of spermine

Yibin Zhou, Hao Tang*, Hanlun Wu, Xiaomei Jiang, Lingyun Wang, Derong Cao*

State Key Laboratory of Luminescent Materials and Devices, School of Chemistry and Chemical Engineering, South China University of Technology, Guangzhou 510641, China

ARTICLE INFO

Article history:
Received 17 March 2023
Revised 24 May 2023
Accepted 29 May 2023
Available online 1 June 2023

Keywords:
Spermine
Pillar[5]arene
Probe
Supramolecular chemistry
Supramolecular cyclization induced emission enhancement

ABSTRACT

Early diagnosis and treatment of cancer requires the development of tools that are both sensitive and selective in detecting spermine. In this study, we presented a "supramolecular cyclization-induced emission enhancement" strategy for the sensitive and selective detection of spermine. A new pillar[5]arene probe (**P1**) demonstrated excellent solution/solid dual-state emission properties, and the addition of certain spermine (Spm) resulted in fluorescence enhancement due to the synergy of multiple weak interactions that restricted the free motion of **P1** in the **P1**⊃Spm complex. This mechanism was further confirmed by time-resolved spectroscopy, DFT calculations, and IGM analysis. With its low limit of detection and high selectivity, **P1** is a promising tool for measuring spermine in artificial urine samples.

Spermine (Spm) is a polyamine widely present in eukaryotic cells and bodily fluids, playing a critical role in cell proliferation and development [1–3]. Recent studies have linked elevated levels of spermine to the presence of cancer, making it a promising biomarker for early detection and efficacy evaluation of cancer treatment [4,5]. However, conventional detection methods such as chromatography and immunoassays are time-consuming and expensive [6,7], necessitating the development of a swift and accurate diagnostic tool. Fluorescent probes have been recognized as a potent approach for spermine detection, with various organic molecules [8–13], quantum dots [14], conjugated polymers [15–17], organic metal compounds [18,19], and supramolecular self-assemblies [20–25] being employed in the past decade. However, the development of novel fluorescent probes for its detection remains desired because the probes for the identification of spermine with high selectivity are still rare.

Pillar[5]arene has been extensively employed in supramolecular chemistry due to its rigid structure and favorable host-guest characteristics [26–33]. By altering its structure, functionalized pillar[5]arenes have been developed and used for the detection of ions and small molecules [34–39]. Recently, we designed a functionalized pillar[5]arene with aggregation-induced emission (AIE) group and multiple-binding-site for the selective discrimination of specific alkylenediamines [40]. Here we proposed a “supramolecular cyclization-induced emission enhancement” (SCIEE) strategy for the selective detection of spermine. By introducing multiple binding sites to pillar[5]arene as a new host (**P1**), **P1** and spermine can form a host-guest complex with a ring-like structure by supramolecular cyclization. Such a ring-like self-assembly restricts the free motion of the host, resulting in the fluorescence enhancement and selective detection of spermine.

In this study, two modified versions of pillar[5]arene (**P1** and its control counterpart **P2**, Scheme 1) were designed and synthesized for the purpose of sensing spermine. Due to the inclusion of diphenylethene groups, both **P1** and **P2** exhibited strong emission properties in both dilute solutions and solid state, featuring dual state emission. **P1** was designed with three binding sites specifically suited for spermine, with the distance between two carboxyl groups of **P1** matching the alkyl chain length of spermine. This design activated the supramolecular cyclization upon the addition of spermine, restricting the free motion of **P1** in the host-guest complex and resulting in enhanced fluorescence. However, **P2** was not effective in recognizing spermine despite also having three binding sites, as the distance between two carboxyl groups of **P2** was too great for the amino groups at the end of the spermine to bind to them simultaneously.

The synthetic route of **P1** and **P2** was shown in Scheme S1 (Supporting information). Initially, intermediates **6a** and **6b** were produced through the Suzuki reaction of compounds **2**/**4** and **5**, respectively. These intermediates were subjected to a sequence of

* Corresponding authors.
E-mail addresses: haotang@scut.edu.cn (H. Tang), drcao@scut.edu.cn (D. Cao).

https://doi.org/10.1016/j.cclet.2023.108626
1001-8417/

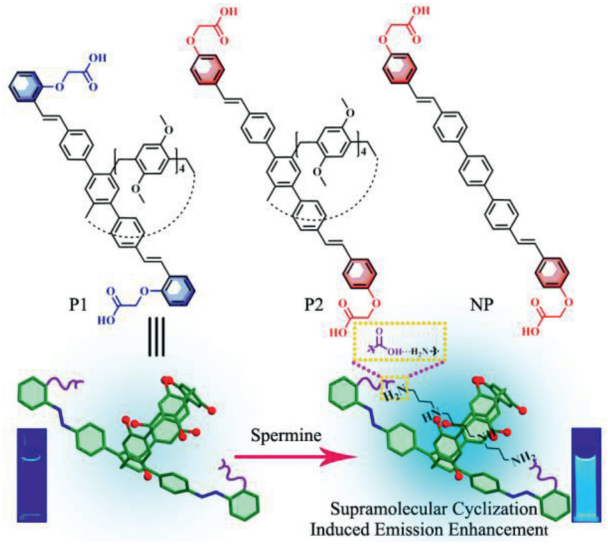

Scheme 1. Chemical structures of **P1**, **P2**, and **NP** and the schematic illustration of detection mechanism.

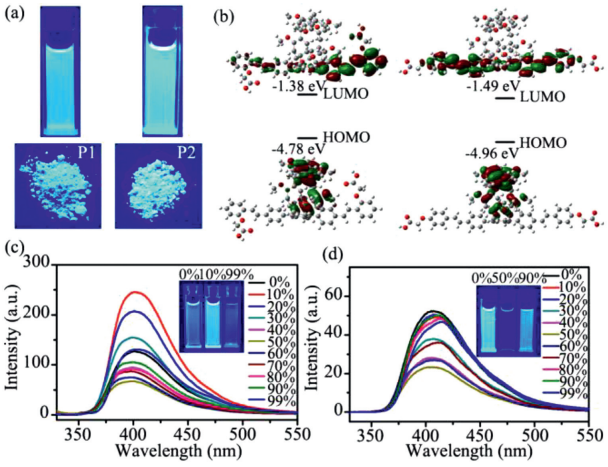

Fig. 1. (a) Photos of the fluorescence emitted by **P1** and **P2** in solution and the solid state; (b) Spatial distribution of the HOMO and LUMO of **P1** and **P2**. Fluorescence spectra of **P1** (c) and **P2** (d) (2.5 μmol/L) in DMSO/H_2O mixtures with varying water content ranging from 0 to 99%.

Williamson and hydrolysis reactions to obtain the desired **P1** and **P2** compounds. NMR and HRMS analysis were conducted to fully characterize the related compounds, as shown in Figs. S1-S25 (Supporting information).

The photophysical characteristics of **P1** and **P2** were examined in acetonitrile and solid states. The absorption spectra of **P1** and **P2** were similar with two absorption bands being observed at *ca.* 305 and 331 nm (Fig. S26a in Supporting information). Similarly, the normalized fluorescence spectra of both compounds were nearly indistinguishable, with blue emission at 397 nm (Fig. 1a and Fig. S26b in Supporting information). DFT calculations indicated that the photophysical properties of **P1** and **P2** were nearly identical due to their comparable conjugated structures and energy gaps (Fig. 1b and Fig. S27 in Supporting information). Additionally, the emission of **P1** and **P2** showed weak solvatochromic properties, with a redshift of 16 and 20 nm, respectively, from toluene to DMF (Fig. S28 and Table S1 in Supporting information).

In the solid state, both **P1** and **P2** emitted strong blue emission at *ca.* 413 and 415 nm, respectively (Fig. S29 in Supporting information). To investigate their fluorescence properties in the aggregated state, dimethyl sulfoxide and water were chosen as the good solvent and poor solvent, respectively. In a dimethyl sulfoxide solution, **P1** (2.5 μmol/L) exhibited blue emission at 401 nm. The fluorescence intensity of the mixture solution showed a tendency to increase and then decrease with the increase of water volume fraction (f_w). However, the magnitude of the fluorescence change was not significant for all samples, and all samples emitted strong blue light (Fig. 1c and Fig. S30a in Supporting information). Similarly, **P2** also displayed significant blue fluorescence in both the solution and aggregated state (Fig. 1d and Fig. S30b in Supporting information). These findings demonstrate that **P1** and **P2** possess excellent solvent/solid dual state emission properties. The large conjugated structure of both compounds enables efficient fluorescence in dilute solutions, while the presence of the pillar[5]arene structure prevents the formation of π-π stacking in the aggregated state, resulting in excellent fluorescence performance of the aggregates.

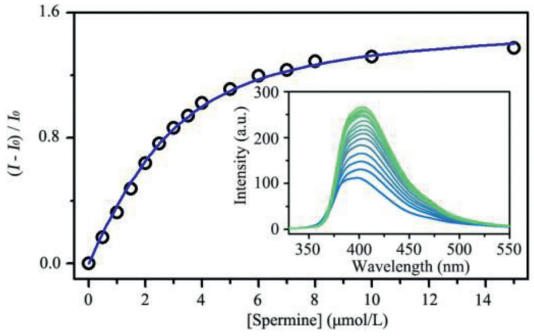

Fig. 2. Binding isotherm of **P1**⊃Spm complex fitted with a 1:1 binding model. Inset: Dependence of fluorescence of **P1** on the concentration of spermine in acetonitrile. [**P1**] = 2.5 μmol/L.

Furthermore, solution-thickening experiments were conducted to confirm whether fluorescence enhancement could be attained by limiting the free motion of **P1** and **P2**. As depicted in Fig. S31 (Supporting information), the fluorescence of both **P1** and **P2** underwent a significant enhancement as the volume fraction of glycerol increased, indicating that the intramolecular rotation of **P1** and **P2** could be constrained by the thickening approach, resulting in an increase in fluorescence.

The host–guest complexation between **P1** and spermine was investigated in acetonitrile. The emission of **P1** was significantly increased upon the addition of spermine (Fig. S32 in Supporting information). The observed fluorescence enhancement correlated with the results of time-resolved spectroscopy experiments, where the fluorescence lifetime of **P1** was found to increase from 2.80 ns to 3.14 ns upon the addition of spermine, as shown in Fig. S33 and Table S2 (Supporting information). To quantify the host-guest binding, a fluorescence titration experiment was conducted with the concentration of **P1** held constant. As depicted in Fig. 2, the fluorescence intensity of **P1** increased gradually with the addition of spermine. The binding isotherms were fitted well to a 1:1 binding model using the Scientist 3 program. The equilibrium binding constant of **P1** to spermine was determined to be $(7.7 \pm 0.6) \times 10^5$ L/mol in acetonitrile. In order to examine the solvent effect on the **P1**-spermine binding, we investigated the fluorescence response of **P1** (2.5 μmol/L) upon adding 5 μmol/L spermine in various solutions, including an acetonitrile/water mixture (1:9, v/v), an aqueous solution, and PBS buffer solutions (pH 6.5 and 7.4). As shown in Fig. S34 (Supporting information), the fluorescence of the **P1** solution barely changed when spermine was added to the aqueous solution or PBS buffer solution, indicating that the binding capacities of **P1** to spermine were not high in those media. The fluorescence enhancement of **P1** was observed in the acetonitrile/water mixture (1:9, v/v) with the equilibrium binding constant of **P1** to spermine determined to be $(2.3 \pm 0.2) \times 10^4$ L/mol,

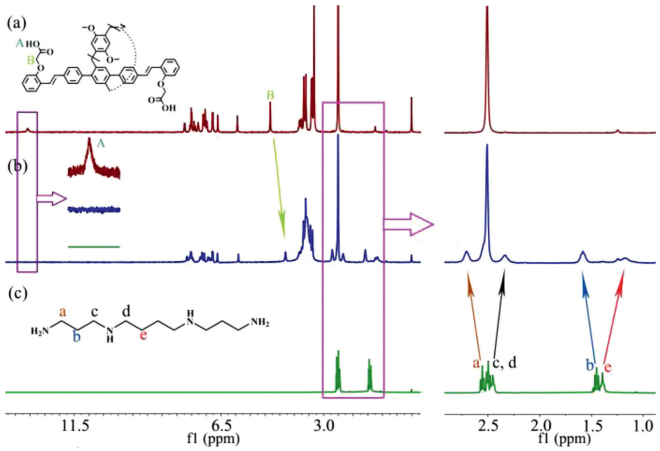

Fig. 3. ^{1}H NMR spectra for the binding of **P1** with spermine (400 MHz, DMSO–d_6). (a) **P1** (5 mmol/L); (b) **P1** (5 mmol/L) and spermine (5 mmol/L); (c) spermine (5 mmol/L).

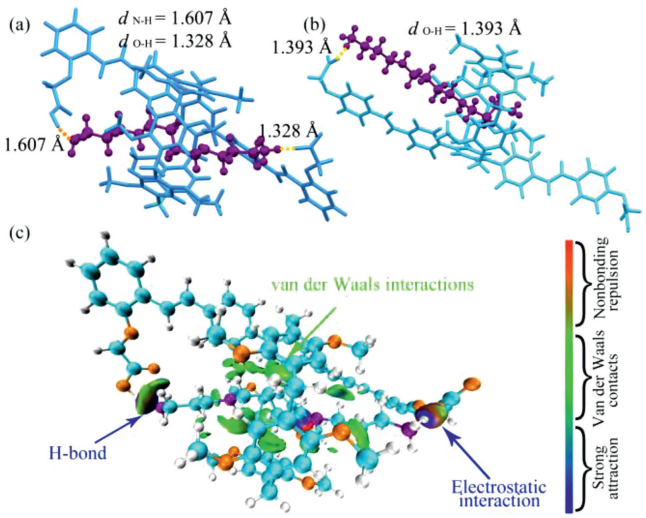

Fig. 4. The complex structure of **P1**⊃Spm (a) and **P2**⊃Spm (b) predicted by DFT calculation. (c) $\delta g^{inter} = 0.01$ a.u. isosurfaces graphs of **P1**⊃Spm.

which is 33 times lower than that in acetonitrile (Fig. S35 in Supporting information). The binding capacity of **P1** to spermine decreased greatly in the presence of water, which may be attributed to the competition between spermine and water for the binding of carboxylic unit of **P1** and high solubility of spermine in water.

To confirm the host-guest interactions between **P1** and spermine, ^{1}H NMR was conducted (Fig. 3). The disappearance of the peak of protons H_A on the carboxyl group of **P1** indicated a proton exchange process between **P1** and spermine, while upfield shifts of the NMR peak was observed for protons H_B on the methylene group. The NMR peaks for protons H_c, H_d, and H_e on spermine displayed substantial upfield shifts and broadening, which were attributed to the inclusion-induced shielding effects and complexation dynamics [41]. Comparatively, the NMR peaks for protons H_a and H_b on spermine exhibited downfield shifts, possibly due to the effect of protonation of the amino group and the inability of the cavity of **P1** to fully encapsulate spermine, leaving the exposed H_a and H_b protons outside the cavity. Besides, ^{1}H NMR titration experiments were performed to further investigate the binding between **P1** and spermine where DMSO was used as the solvent instead of acetonitrile due to **P1**'s inadequate solubility in acetonitrile for NMR experiments (Fig. S36 in Supporting information). The chemical shifts of protons on spermine were shifted with the addition of **P1** and the binding isotherm was fit well with a 1:1 binding model, suggesting a 1:1 host-guest binding. The equilibrium binding constant of **P1** to spermine in DMSO was calculated to be $(5.3 \pm 0.8) \times 10^3$ L/mol using the Scientist 3 program (Fig. S37 in Supporting information). Additionally, an ESI-MS experiment was conducted, which also revealed the formation of 1:1 host-guest complex in the **P1**/Spm system, as evidenced by the presence of the [**P1**⊃Spm]$^+$ peak in the spectrum (Fig. S38 in Supporting information).

The control experiments were conducted by observing the fluorescent behavior of two control molecules of **P1** (*i.e.*, **P2** and **NP**) upon the addition of spermine (Fig. S39 in Supporting information). The absence of substantial fluorescence enhancement in **P2** and **NP** indicated their inability to effectively bind with spermine, which was attributed to the great distance between two carboxyl groups of **P2** and the lack of a pillar[5]arene cavity in **NP**. This finding reinforced the importance of the pillar[5]arene cavity and the dual carboxyl-amine interactions in the selective recognition of spermine.

To further investigate the mechanism behind **P1**'s selective recognition of spermine, several methods were employed, including DFT calculations and independent gradient model (IGM) analysis. The complex structure of **P1**⊃Spm was optimized by DFT and depicted in Fig. 4a. One binding site showed a strong electrostatic interaction (1.328 Å) between the carboxylate anion and the alkylammonium cation due to proton transfer from a carboxyl group of **P1** to an amino group of spermine. At another binding site, an O–H···N bond (1.607 Å) was formed between a carboxyl group of **P1** and an amine group of spermine, consistent with the characteristics of carboxyl-amine interaction, namely, charge-assisted hydrogen bond [42]. IGM analysis revealed strong electrostatic interaction, hydrogen bond (indicated by blue areas in the isosurfaces), and van der Waals interactions (indicated by green areas in the isosurfaces) between **P1** and spermine (Fig. 4c) [43]. In contrast, the amino groups at the end of spermine could not attach to two **P2** carboxyl groups simultaneously to establish two carboxyl-amine interactions, as shown in Fig. 4b. These theoretical studies confirmed that the synergy of carboxyl-amine interactions and van der Waals interactions between the host and the guest played a key role in restricting the free motion of **P1** and achieving supramolecular cyclization-induced emission enhancement.

The investigation of the selectivity of **P1** towards spermine in the presence of various amines was carried out. Firstly, 1,12-diaminododecane, which has the same chain length as spermine, was chosen to bind to **P1**. As shown in Fig. S40 (Supporting information), the emission of **P1** was significantly increased upon the addition of 1,12-diaminododecane, indicating that the presence of 1,12-diaminododecane may cause interference in the detection of spermine. However, 1,12-diaminododecane is not biogenic amine and not typically present in the physiological environment and is therefore unlikely to cause interference in the detection of spermine [44]. Thus, taking into account practical application scenarios, interference was mainly selected from some common biogenic amines. Secondly, the results presented in Fig. 5 showed that the fluorescence emission of **P1** was significantly enhanced upon the addition of spermine, while no significant increase in fluorescence was observed in any of the other biogenic amine solutions. Thirdly, considering that spermine is a basic compound, the impact of NH_3 on the spermine sensing process was investigated. As depicted in Fig. S41 (Supporting information), **P1** was capable of accurately detecting spermine in the presence of varying concentrations of NH_3. Additionally, competition experiments were conducted to evaluate **P1**'s ability to distinguish spermine from other amines, as shown in Fig. S42 (Supporting information). The experimental findings indicated that **P1** exhibited selective detection of spermine and

Table 1
Real sample analysis data for different samples pre-spiked with the known concentrations of spermine.

Sample	Prepared (μmol/L)	Found (μmol/L)	Recovery (%)	RSD (%, $n=3$) [a]
Artificial urine with spermine	3	3.18	106	0.91
	5	4.82	96	2.28
	9	9.42	105	2.84

[a] Relative standard deviation.

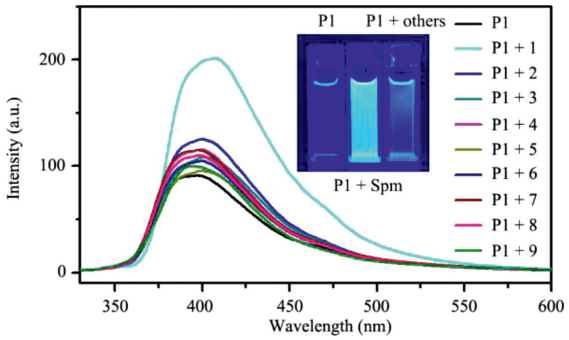

Fig. 5. The fluorescence spectra of **P1** (2.5 μmol/L) with different biogenic amines (5 μmol/L) in acetonitrile. Inset: photographs of samples under 365 nm UV illumination. Guests are 1: Spermine, 2: Spermidine, 3: 1,5-pentanediamine, 4: 1,4-butanediamine, 5: Tryptamine, 6: Histamine, 7: Tyramine, 8: Urea, 9: Ethylenediamine.

was barely influenced by basic compounds. The limit of detection (LOD) for spermine in acetonitrile was determined as 0.094 ± 0.002 μmol/L using the equation $3\sigma/S$ (where standard deviation, $\sigma = 1.1$ and slope, $S = 3.5 \times 10^7$) (Fig. S43 in Supporting information) [20]. These results indicated that **P1** possessed high sensitivity and selectivity in recognizing spermine, placing it among the most selective and sensitive probes (Table S3 in Supporting information).

To showcase the potential utility of **P1** in detecting spermine in artificial urine, the fluorescence spectra of **P1** were determined with the addition of artificial urine (depicted in Fig. S44a in Supporting information). The results showed that the fluorescence intensities at 400 nm were linearly proportional to the spermine concentration in the range of 0–17 μmol/L, as demonstrated in Fig. S44b (Supporting information). The LOD for spermine in artificial urine was determined to be 0.4 μmol/L, which is sensitive enough in pathological conditions. The findings of the recovery experiments are summarized in Table 1.

In conclusion, we used supramolecular cyclization induced emission enhancement as a new strategy to detect spermine by pillar[5]arene derivative (*i.e.*, **P1**) bearing three binding sites for spermine. An increase in the fluorescent emission of **P1** with the addition of spermine was attributed to the inhibition of **P1**'s free motion in the **P1**⊃Spm complex by supramolecular cyclization, aided by multiple weak interactions. **P1** possessed high sensitivity and selectivity in recognizing spermine (with LOD of 0.094 μmol/L and 0.4 μmol/L for spermine in acetonitrile and artificial urine) due to the synergism based on the pillar[5]arene cavity, the dual carboxyl-amine interactions, and the proper chain lengths of **P1** and spermine, placing it among the most selective and sensitive probes. However, a similar pillar[5]arene derivative **P2** cannot form such a ring-like structure by supramolecular cyclization, resulting no obvious emission enhancement because the chain length of **P2** does not match that of spermine. Another similar probe **NP** does not show the supramolecular cyclization-induced emission enhancement due to the lack of a pillar[5]arene cavity. This study presents a novel approach to developing probes for spermine detection, and suggests potential applications in early cancer diagnosis. However, it should be mentioned that other alkanediamines with similar chain lengths, *i.e.*, 1,12-diaminododecane may increase the emission of **P1**. Fortunately, 1,12-diaminododecane is not biogenic amine and therefore may not interfere the detection of spermine in the physiological environment samples.

Declaration of competing interest

The authors declare that they have no known competing financial interests or personal relationships that could have appeared to influence the work reported in this paper.

Acknowledgments

This work was supported by the National Natural Science Foundation of China (Nos. 22071066, 22071065), the National Key Research and Development Program of China (No. 2016YFA0602900), the Guangdong Natural Science Foundation, China (No. 2018B030311008), and the Guangzhou Science and Technology Project, China (No. 202102020802).

Supplementary materials

Supplementary material associated with this article can be found, in the online version, at doi:10.1016/j.cclet.2023.108626.

References

[1] C. Stefanelli, F. Bonavita, I. Stanic, et al., FEBS Lett. 437 (1998) 233–236.
[2] A. Bibillo, M. Figlerowicz, R. Kierzek, Nucl. Acids Res. 27 (1999) 3931–3937.
[3] C. Moinard, L. Cynober, J.-P. de Bandt, Clin. Nutr. 24 (2005) 184–197.
[4] R.A. C.asero, L.J. M.arton, Nat. Rev. Drug. Disc. 6 (2007) 373–390.
[5] D.H. Russell, Nat. New Biol. 233 (1971) 144–145.
[6] H.E. Flores, A.W. Galston, Plant Physiol. 69 (1982) 701–706.
[7] Y. Ma, G. Liu, M. Du, et al., Electrophoresis 25 (2004) 1473–1484.
[8] J.T. Fletcher, B.S. Bruck, Sens. Actuators B: Chem. 207 (2015) 843–848.
[9] B. Lee, R. Scopelliti, K. Severin, Chem. Commun. 47 (2011) 9639–9641.
[10] W. Li, L. Wang, T. Sun, et al., Commun. Biol. 4 (2021) 803.
[11] H. Nohta, H. Satozono, K. Koiso, et al., Anal. Chem. 72 (2000) 4199–4204.
[12] L. Wang, S. Xin, C. Zhang, et al., J. Mater. Chem. B 9 (2021) 9383–9394.
[13] M. Barros, S. Ceballos, P. Arroyo, et al., Chemosensors 10 (2021) 8.
[14] S.M. T.awfik, J. Shim, D. Biechele-Speziale, et al., Sens. Actuators B: Chem. 257 (2018) 734–744.
[15] B. Bao, L. Yuwen, X. Zheng, et al., J. Mater. Chem. 20 (2010) 9628–9634.
[16] A. Satrijo, S.E. Kooi, T.M. Swager, Macromolecules 40 (2007) 8833–8841.
[17] J. Wang, Q. Zhang, Z. De Liu, et al., Analyst 137 (2012) 5565–5570.
[18] C.F. Chow, M.H. L.am, W.Y. W.ong, Anal. Chem. 85 (2013) 8246–8253.
[19] G. Munzi, S. Failla, S. Di Bella, Analyst 146 (2021) 2144–2151.
[20] A.A. B.hosle, M. Banerjee, N. Barooah, et al., J. Photochem. Photobiol. A: Chem. 426 (2022) 113770.
[21] Z. Kostereli, K. Severin, Chem. Commun. 48 (2012) 5841–5843.
[22] B. Lu, L. Wang, X. Ran, et al., Biosensors 12 (2022) 633.
[23] H. Tian, X. Yu, J. Yao, et al., Chem. Commun. 57 (2021) 1806–1809.
[24] J. Tu, S. Sun, Y. Xu, Chem. Commun. 52 (2016) 1040–1043.
[25] G. Jiang, W. Zhu, Q. Chen, et al., Sens. Actuators B: Chem. 261 (2018) 602–607.
[26] X.Y. Lou, Y.W. Y.ang, Adv. Mater. 32 (2020) 2003263.
[27] K. Wang, J.H. Jordan, K. Velmurugan, et al., Angew. Chem. Int. Ed. 60 (2021) 9205–9214.
[28] K. Wang, X. Tian, J.H. J.ordan, et al., Chin. Chem. Lett. 33 (2022) 89–96.
[29] L. Wu, C. Han, X. Jing, et al., Chin. Chem. Lett. 32 (2021) 3322–3330.
[30] L. Xu, Z. Wang, R. Wang, et al., Angew. Chem. Int. Ed. 59 (2020) 9908–9913.
[31] W.L. Zhou, Y. Chen, W. Lin, et al., Chem. Commun. 57 (2021) 11443–11456.
[32] H. Zhu, Q. Li, L.E. Khalil-Cruz, et al., Sci. China Chem. 64 (2021) 688–700.
[33] L. Xu, R. Wang, H. Tang, et al., J. Mater. Chem. A 10 (2022) 11332–11339.

[34] J. Chen, H. Ni, Z. Meng, et al., Nat. Commun. 10 (2019) 3546.
[35] D. Dai, Z. Li, J. Yang, et al., J. Am. Chem. Soc. 141 (2019) 4756–4763.
[36] X. Jiang, L. Wang, X. Ran, et al., Biosensors 12 (2022) 571.
[37] Q. Lin, Z.H. Wang, T.T. Huang, et al., J. Mater. Chem. C 9 (2021) 3863–3870.
[38] Y. Luo, W. Zhang, Q. Ren, et al., Chin. Chem. Lett. 33 (2022) 5120–5123.
[39] D. Cao, H. Meier, Chin. Chem. Lett. 30 (2019) 1758–1766.
[40] Y. Zhou, H. Tang, Z.H. L.i, et al., Chem. Commun. 57 (2021) 13114–13117.
[41] X. Shu, S. Chen, J. Li, et al., Chem. Commun. 48 (2012) 2967–2969.
[42] P. Gilli, L. Pretto, V. Bertolasi, et al., Acc. Chem. Res. 42 (2009) 33–44.
[43] T. Lu, F. Chen, J. Comput. Chem. 33 (2012) 580–592.
[44] N. Kaur, S. Chopra, G. Singh, et al., J. Mater. Chem. B 6 (2018) 4872–4902.